

NLRP3 Inflammasome Upregulates PD-L1 in Ovarian Cancer and Contributes to an Immunosuppressive Microenvironment

Wenjing Pan^{1,*}, Zhaoyang Jia^{1,*}, Jingtong Du^{1,*}, Kexin Chang², Yiming Liu², Wei Liu¹, Xibo Zhao³, Wenhua Tan¹

¹Department of Gynecology, The Second Affiliated Hospital of Harbin Medical University, Harbin, Heilongjiang, 150081, People's Republic of China;

²Department of Gynecology Oncology, Harbin Medical University Cancer Hospital, Harbin, Heilongjiang, 150081, People's Republic of China;

³Department of Gynecological Oncology, Sun Yat-Sen Memorial Hospital of Sun Yat-Sen University, Guangzhou, 510120, People's Republic of China

*These authors contributed equally to this work

Correspondence: Xibo Zhao; Wenhua Tan, Email zhaoxb8@mail.sysu.edu.cn; tanwenhua1962@126.com

Introduction: The NLRP3 inflammasome has been implicated in the initiation of inflammation and tumorigenesis; however, its role in epithelial ovarian cancer (EOC) remains unclear.

Methods: This study employed high-throughput sequencing data, ELISA, clone formation assay, Western blot, and flow cytometric analysis to investigate the specific role of the NLRP3 inflammasome in EOC.

Results: NLRP3 was highly expressed in human EOC tissues and correlated with an unfavorable prognosis. Activation of the NLRP3 inflammasome by LPS and ATP promoted EOC cell proliferation and increased IL-1 and PD-L1 levels. MCC950, a NLRP3 inflammasome blocker, reduced IL-1 and PD-L1 levels and diminished tumor-immune suppressive cells, such as myeloid-derived suppressor cells (MDSCs), tumor-associated macrophages (TAMs), and PD-1⁺ CD4⁺ T cells, in a murine model of ovarian cancer. This intervention also suppressed tumor growth.

Conclusion: Our investigation revealed the pro-tumorigenic role of the NLRP3 inflammasome and its regulation of PD-L1 expression in EOC. Blockade of the NLRP3 inflammasome led to reduced PD-L1 expression, fewer immunosuppressive cells, and suppressed tumor growth. These findings suggest that targeting the NLRP3 inflammasome-PD-L1 axis could be a novel treatment approach for ovarian cancer.

Keywords: NLRP3 inflammasome, PD-L1, immunosuppressive cells, EOC, inflammation

Introduction

Ovarian cancer is among the most prevalent gynecological malignancies, accounting for approximately 240,000 new diagnoses globally each year and rising.¹ The underlying molecular mechanisms of ovarian cancer development remain elusive, and it is the sixth leading cause of death for female cancers.² Therefore, identifying a potent therapeutic target is crucial to combat the bleak prognosis of ovarian cancer.

Research indicates a connection between the immune system and the prognosis of ovarian cancer.³ The tumor microenvironment (TME) of ovarian cancer is complex and includes immune suppressive cells such as TAMs, MDSCs, and Tregs.³ These cells contribute to an immunosuppressive TME, which influences disease progression and response to therapy.⁴ Inflammatory processes could also interact with oncogenic alterations to increase the risk of tumorigenesis.⁵ Chronic inflammation is considered a major contributor to ovarian cancer pathogenesis.⁶ The inflammasome regulates the innate immune response, protecting the organism from infections; however, excessive activation may trigger a dysregulated inflammatory response leading to tissue damage and malignancy.⁷

The NLRP3 inflammasome, as the prototypical member of inflammasomes, is primarily composed of NOD-like receptor family protein NLRP3, adaptor protein ASC, and pro-caspase-1. A range of stimuli, including dsRNA, ATP, and asbestos, have the potential to trigger NLRP3 inflammasome activation.⁸ Another requirement is the presence of a danger-associated molecular pattern (DAMP), such as lipopolysaccharide (LPS).⁹ Upon activation of NLRP3, an assembly involving ASC and pro-Caspase-1 takes place, resulting in the formation of the NLRP3 inflammasome complex.¹⁰ The activation of the NLRP3 inflammasome triggers the maturation of IL-1 β and IL-18, inducing inflammatory responses and cell death.¹¹ NLRP3 inflammasome has a dual role in tumors,⁷ with protective roles in hepatocellular and colorectal carcinoma,^{12,13} that lower NLRP3 levels are associated with poorer prognosis and higher morbidity. However, NLRP3 inflammasome facilitates tumor progression in various cancers, including breast as well as head and neck cancer.^{14,15} The PD-L1-NLRP3 inflammasome has been identified as a tumor-intrinsic signaling pathway in melanoma that contributes to resistance to anti-PD-1 immunotherapy;¹⁶ Therapeutic targeting of NLRP3 inhibits tumor development and reprograms the MDSC compartment.¹⁷ MDSCs, believed to prevent anti-tumor immune response,¹⁸ can be divided into two subsets: monocytic MDSC (M-MDSC) (labeled CD11b⁺ LY6G⁻ LY6C^{high}) and granulocytic polymorphonuclear MDSC (PMN-MDSC) (labeled CD11b⁺ LY6G⁺ LY6C^{low}). While both subsets play crucial roles in cancer, the granulocytic subset is preferentially expanded in most tumors.¹⁹ Inhibition of the NLRP3 inflammasome in MDSCs using gold nanoparticles improves PD-1 tumor immunotherapy.²⁰ Additionally, a few studies propose that the NLRP3 inflammasome may be involved in the malignant transformation of endometriosis-associated ovarian carcinoma, a subtype of EOC.^{21,22} However, the exact function and mechanism of NLRP3 inflammasome in ovarian cancer remain unknown.

This study aims to examine the role of NLRP3 inflammasome in ovarian cancer. As EOC accounts for over 95% of ovarian cancer cases, we analyzed NLRP3 expression in EOC tissues and its relation to the tumor microenvironment and immune checkpoint molecules. We then showed the oncogenic role of NLRP3 inflammasome and its connection to PD-L1 in EOC cell lines and mice models, which may provide a new treatment target for ovarian cancer.

Methods

Data Selection and Survival Analysis

The EOC expression data were obtained from TCGA (<https://portal.gdc.cancer.gov/>). The GDC portal was used to download the expression files for the probes, which were then mapped to gene names using the Ensembl database. TMM normalization was performed using edgeR, and CPM values were calculated. After removing samples lacking survival data or with survival times shorter than 30 days, a total of 362 samples from the TCGA dataset were included in this analysis. To assess the impact of NLRP3 differential expression on ovarian cancer prognosis, the samples were divided into high- and low-expression groups, and Kaplan-Meier (KM) analysis was performed using “survminer” and “survival”. Disease-free survival (DFS), progression-free survival (PFS), and overall survival (OS) were analyzed in the two groups.

Recognition and Portrayal of Immune Function in EOC

To understand the role of NLRP3 in the tumor microenvironment (TME) of EOC, we utilized the Estimation of STromal and Immune cells in Malignant Tumour tissues using Expression data (ESTIMATE) method (<https://doi.org/10.1038/ncomms3612>). This method enables the calculation of stromal and immune scores from tumor sample gene expression profiles, indicating stromal and immune cell abundance, respectively, with summing both scores providing the ESTIMATE score, a measure of tumor purity.²³ We employed the GSEA software to evaluate NLRP3 differential expression signaling pathway enrichment with background genes from the molecular signature library MSigDB (<http://www.gseamsigdb.org/gsea/downloads.jsp>), with the subset (c2.cp.kegg.v7.4.symbols.gmt). Additionally, we analyzed NLRP3 correlation with immune checkpoints using the Pearson algorithm.

Cell Culture and Reagents

The human EOC cell lines SKOV3, A2780, OVCAR3, OVCAR5, OV90, HO8910, and ES2, as well as the human normal ovarian epithelial cell IOSE80, were kindly provided by the Experimental Center at the Second Affiliated Hospital of

Harbin Medical University. The use of these cell lines was approved by the Ethics Committee of the Second Affiliated Hospital of Harbin Medical University, and all cell lines were authenticated by STR profile. All cells were cultured at 37°C in a humidified atmosphere containing 5% CO₂. OVCAR3 and OV90 were cultured in DMEM with High Glucose (VivaCell, China), while SKOV3, A2780, OVCAR5, HO8910, ES2, and IOSE80 were cultured in RPMI-1640 medium (Gibco, USA). Both media were supplemented with 10% Fetal Bovine Serum (Gibco, USA) and 1% penicillin-streptomycin (Biosharp, China). The mouse ovarian cancer cell line ID8 (iCell Bioscience Inc., Shanghai, China) was cultured in DMEM with High Glucose (VivaCell, China) following the manufacturer's instructions. LPS, ATP and MCC950 were purchased from MedChemExpress (Monmouth Junction, NJ, USA). The following antibodies were utilized in this study: Rabbit Polyclonal anti-NLRP3 (CY5651), Rabbit Monoclonal anti-PD-L1 (CD274) Antibody (Abways, Shanghai, China; CY5980-20); Rabbit Polyclonal anti-Cleaved-Caspase-1(p20) (YC0022-20), Rabbit Polyclonal anti-IL-1 β (YT5201), Rabbit Polyclonal anti-CXCL2(YT7842-20) (ImmunoWay Biotechnology, Plano, TX, USA).

Syngeneic Tumor Modelling and Inflammasome Activation

Four-week-old female C57BL/6N mice, weighing 16–18g on average, were purchased from the Animal Experiment Center of the Second Affiliated Hospital of Harbin Medical University. The animal experimentation procedures were conducted in strict accordance with the Guideline for Ethical Review of Animal Welfare (GB/T 35892–2018) established by the People's Republic of China. These procedures were approved by the Animal Ethics Review Committee of the Second Affiliated Hospital of Harbin Medical University. ID8 is a mouse ovarian surface epithelial cell clone of C57BL/6 origin, derived from ovarian carcinoma.²⁴ To establish a syngeneic tumor model, ID8 cells (2×10^7) were subcutaneously injected into C57BL/6N mice. Mice were then randomly divided into two groups once the model was established. The experimental group was injected intraperitoneally with MCC950 (15mg/kg) every 2 days, while the control group received an equivalent amount of PBS. This treatment was maintained for three weeks. The tumor volume (TV) was measured every four days, $TV = 1/2 \times a \times b^2$ (a is length, b is width). Blood, tumor, and spleen samples were collected for further experimentation.

The NLRP3 inflammasome can be activated by LPS and ATP, and inhibited by MCC950.²⁵ SKOV3 cells were initially exposed to LPS (1 μ g/mL) for 6 h. Subsequently, they were pretreated with serum-free medium with DMSO (1:1000) or MCC 950 (10 μ M) for 1h before being stimulated with ATP (5 mM) for 1h.

Western Blot and ELISA

Equal quantities of protein and molecular markers were loaded into SDS-PAGE gel wells. The proteins were then transferred to a PVDF membrane, which was blocked at room temperature (RT) for 2 hours. The membrane was then incubated with the primary antibody of the target protein overnight at 4°C, followed by the addition of the diluted secondary antibody and incubation for 1 h at RT. The membrane was then washed and immersed in ECL luminescent solution to develop the colour for 2 min, after which it was placed on a fully automated chemiluminescence imaging system for scanning. ELISA: The serum levels of IL-1 β in mice were assessed using an ELISA kit (Shanghai Jianglai Industrial Limited By Share Ltd, JL18442-96T), following the procedures outlined in the kit's instructions.

Immunofluorescence (IF)

The cells were fixed with 4% paraformaldehyde at RT for 10–15 minutes, then blocked with 2% BSA for 30 minutes. Next, they were incubated with the primary antibody overnight at 4°C. Afterward, the corresponding fluorescent secondary antibody was added and incubated at 37°C for 1.5 h in the dark. The cells were then stained with DAPI for 10 minutes at RT. Finally, images were captured using a fluorescence microscope.

Immunohistochemistry (IHC)

Ten EOC tissue samples and ten normal ovarian tissue samples were obtained from the Second Affiliated Hospital of Harbin Medical University. The EOC patients were newly diagnosed and untreated before surgery, with all cases having a clear pathological diagnosis. Informed consent was obtained from patients, and the study was approved by the Medical Ethics Committee. For IHC, paraffin-embedded sections were subjected to antigen retrieval, followed by blocking. The

sections were then incubated overnight at 4°C with Rabbit Anti-Human NLRP3 antibody (1:500). Afterward, they were incubated with a secondary antibody (Goat Anti-Rabbit/Mouse IgG [Kit-0038, Nakasugi Jinqiao]) for 30 minutes at RT. Samples were stained with DAB, dehydrated, and sealed. Observations were made using an Olympus microscope, with four randomly selected fields of view per sample. Integrated optical density (IOD) and area were measured using ImageJ software to calculate the average optical density (AOD), using the formula: $AOD = IOD/Area$.

Cck-8

3000 cells were seeded per well in 96-well plates and exposed to varying concentrations of MCC950 (1, 2, 5, 10 μ M). The plates were incubated in a 5% CO₂ incubator at 37°C for 24, 48, and 72 hours. Cell activity was assessed by removing the supernatant, adding 10 μ L/well CCK-8 solution, and incubating for 2 hours. Optical density at 450 nm (OD 450) was measured using the Multiskan FC enzyme marker.

TUNEL and Colony Formation

TUNEL: Cells in each group were fixed with 4% paraformaldehyde at RT after dosing, pretreated with 0.1% Triton X-100, and then incubated with the TUNEL staining solution for 1 hour at 37°C in the dark. Cell nuclei were stained with DAPI and visualized under a fluorescence microscope, then photographed.

Colony formation: 1×10^4 cells were inoculated in 6-well plates with 2 mL of RPMI-1640 medium (Gibco, USA) per well. After six days of treatment with the respective drug, the cells were fixed with 4% paraformaldehyde at RT, stained with crystal violet, photographed, counted, and analyzed.

Flow Cytometry

First, prepare single cell suspensions of spleen and tumour tissue. Add 100 μ L of DMSO to Zombie Aqua and ensure complete dissolution through mixing, and take the prepared cell suspension and perform dead/live staining; stain with the following antibodies according to the proportions specified in the antibody instructions: FITC anti-mouse/human CD11b (BioLegend, Cat. no. 101205), PE/Cyanine7 anti-mouse F4/80 (BioLegend, Cat. no. 123113), APC/Cyanine7 anti-mouse CD4 (BioLegend, Cat. no.100525), PerCP/Cyanine5.5 anti-mouse CD8a (BioLegend, Cat. no. 100733), APC anti-mouse Ly-6G/Ly-6C (Gr-1) (BioLegend, Cat. no. 108411), Brilliant Violet 650™ anti-mouse CD25 (BioLegend, Cat. no. 102038), Brilliant Violet 421™ anti-mouse CD366 (Tim-3) (BioLegend, Cat. no. 119723), Brilliant Violet 785™ anti-mouse CD279 (PD-1) (BioLegend, Cat. no.135225).

Intracellular cytokine staining was performed by adding 2 mL of True-Nuclear™ 1 \times Perm Buffer to the cell suspension, followed by centrifugation at 400–600 g for 5 min at RT. Cells were fixed and permeabilized using the Foxp3/Transcription Factor Staining Buffer Kit (Thermo Fisher Scientific, no. 5523). PE anti-mouse/rat/human FOXP3 (BioLegend, Cat. no. 320007) was added and incubated at 4 °C in the dark for 60min. Stained cells were assessed using a NovoCyte 3110 flow cytometer (Agilent Technologies Co. Ltd.), and flow cytometry data were analyzed by Novo Express1.5.0.

Statistical Analysis

GraphPad Prism 10.1 was used for statistical data processing and visualization. Findings were presented as mean \pm SD; Each experiment was reproduced at least three times with biologically or technically independent replicates, unless otherwise stated. Outcomes between two different groups were compared using a *t*-test or a Wilcoxon rank-sum test. Statistical significance was set at $P < 0.05$.

Results

High Expression of NLRP3 in EOC and Correlates with Poor Prognosis

The TCGA-OV dataset was first used to validate the differential expression of NLRP3 between EOC and normal ovarian samples, showing that NLRP3 was significantly upregulated in EOC ($p < 0.0001$, [Figure 1a](#)). This result was corroborated via immunohistochemistry in EOC ($n=10$) and normal ovarian epithelial tissues ($n=10$) ($p < 0.001$, [Figure 1b](#)). NLRP3

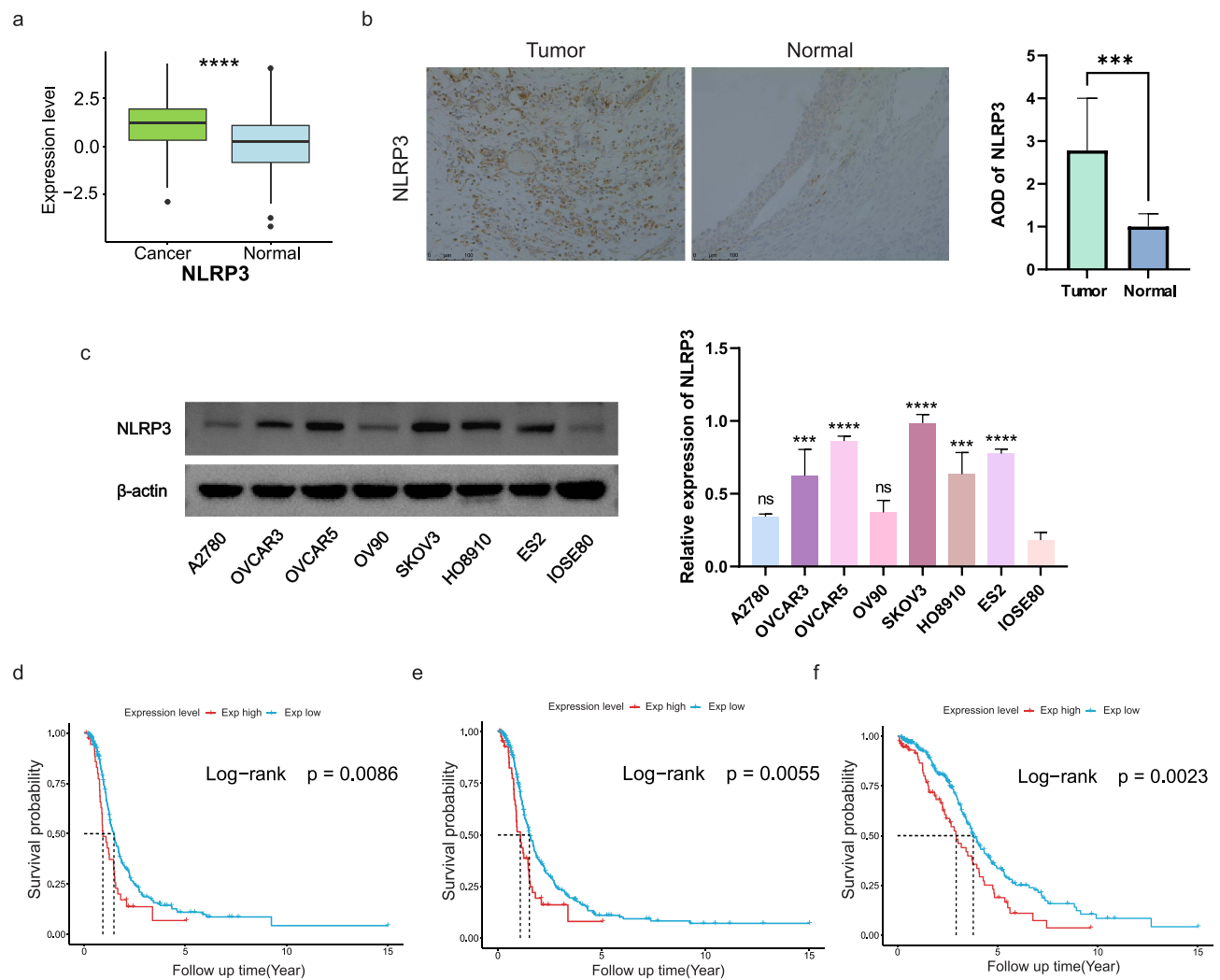


Figure 1 NLRP3 expression in EOC and Kaplan-Meier survival analyses. (a) A box plot showed differential NLRP3 expression in normal and EOC samples. (b) Immunohistochemistry verified NLRP3 expression patterns in normal ovarian epithelial cells (IOSE80) and various EOC tissues (n=10) and their AODs; (c) Representative Western blot image showing NLRP3 protein expression in normal ovarian epithelial cells (IOSE80) and various EOC cell lines. Quantitative analysis of protein expression levels is shown below, with data represented as mean \pm SD from three independent experiments. Symbols indicate statistically significant differences between IOSE80 and ovarian cancer cell lines. (d–f) Kaplan-Meier analysis revealed significant differences in patients' DFS (d), PFS (e), and OS (f) between NLRP3 high and low expression groups in the training cohort. Data are shown as mean \pm SD; ns, no significance; ***, $p < 0.001$; ****, $p < 0.0001$.

protein levels were significantly higher in various ovarian cancer cell lines compared to normal ovarian epithelial cells, with the SKOV3 cell line showing the highest expression (Figure 1c). Furthermore, the impact of NLRP3 differential expression on the prognosis of EOC patients was analyzed using survival curve, showing patients with higher NLRP3 expression had poorer prognosis, including disease-free survival (DFS) (Log-rank $p = 0.0086$, Figure 1d), progression-free survival (PFS) (Log-rank $p = 0.0055$, Figure 1e), and overall survival (OS) (Log-rank $p = 0.0023$, Figure 1f). These findings indicated a critical role for NLRP3 in EOC progression.

Association of NLRP3 with TME and Immune Checkpoints in EOC

Research indicates that NLRP3 is significantly associated with inflammation and immune responses.²⁶ We assessed the relationship between NLRP3 and the ovarian cancer TME using the ESTIMATE algorithm. Our findings indicated a significant positive correlation between elevated NLRP3 expression and stromal, immune, and ESTIMATE scores in EOC samples, while a negative correlation with tumor purity (Figure 2a). This suggests that NLRP3 facilitates immune cell infiltration within the ovarian cancer TME. Further analysis through GSEA of NLRP3-linked signaling pathways

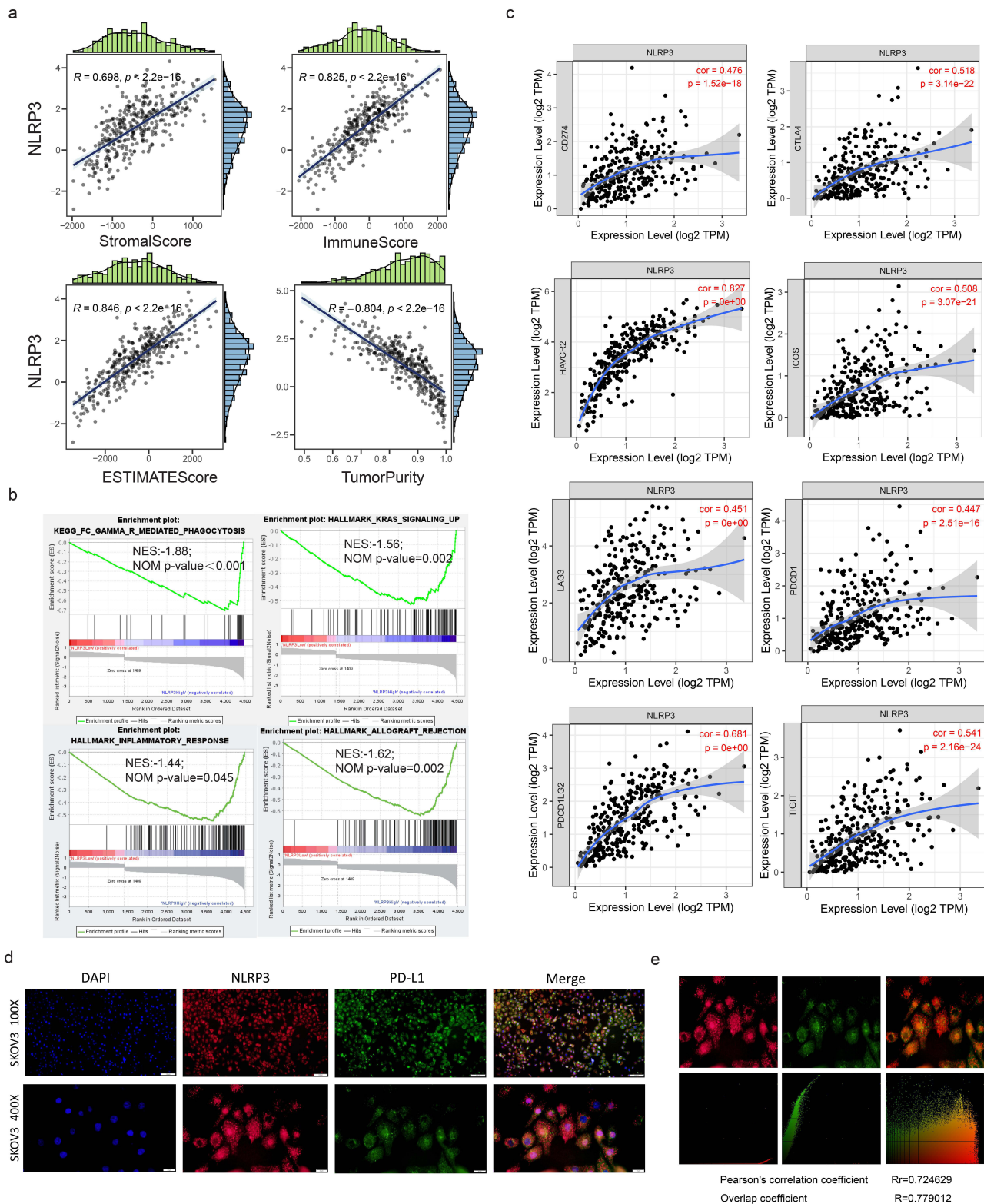


Figure 2 Correlation between NLRP3 and immune infiltration and immune checkpoints. (a) The association of NLRP3 with stromal score, immune score, ESTIMATE score, and tumor purity was analyzed using the ESTIMATE algorithm. (b) The correlation between NLRP3 expression levels and signaling pathways enriched in EOC was analyzed by GSEA. (c) Scatter diagrams showed the correlation between NLRP3 and multiple immune checkpoints in EOC. (d) Representative immunofluorescence images from three independent experiments of NLRP3 and PD-L1 subcellular localization in the SKOV3 cell line. Nuclei were stained blue (DAPI), NLRP3 red, and PD-L1 green. (e) Pearson correlation analysis analyzed fluorescence co-localization of NLRP3 and PD-L1.

demonstrated an inverse relationship between high NLRP3 expression and pathways such as FcγR-mediated phagocytosis by macrophages, inflammatory responses, KRAS signaling, and allograft rejection (Figure 2b). These results imply that NLRP3 expression may have a suppressive effect on immune responses in EOC. To delve deeper into the role of NLRP3 in EOC, Pearson's correlation analysis was utilized to examine the connection between NLRP3 and immuno-checkpoints. The results showed a positive correlation between NLRP3 expression and several immuno-checkpoint markers, including CD274 (PD-L1), LAG3, and others (Figure 2c). While PD-L1 and NLRP3 showed a moderate correlation ($\text{cor}=0.476$, $p = 1.52\text{e-}18$, Figure 2c), it has been shown that PD-L1 and NLRP3 could interact with each other, influencing the TME and thus the immune response or the efficacy of immunotherapy in certain malignancies.^{16,20} Therefore, PD-L1 was chosen for further investigation. An immunofluorescence assay confirmed NLRP3 and PD-L1 protein expression in SKOV3 cell lines, with the former predominantly found in the cytoplasm and the latter in the cell membrane and cytoplasm (Figure 2d). The two proteins exhibited a strong correlation (Pearson's $R_r = 0.724629$) by immunofluorescence co-localization analysis (Figure 2e), consistent with previous findings in hepatocellular carcinoma.²⁶

Activation of the NLRP3 Inflammasome in the SKOV3 Cell Line Enhanced PD-L1 Expression

Our following investigation focused on the role of NLRP3 inflammasome in the SKOV3 cell line, which exhibited the highest NLRP3 expression levels. Cells were treated with varying concentrations of MCC950 for 24 hours, with a control group left untreated. CCK-8 assays showed a significantly decreased SKOV3 cell proliferation rate in the presence of 10 μM MCC950 compared to the control group ($p < 0.05$, Figure 3a). Next, this study validated the activation effect of LPS combined with ATP on the NLRP3 inflammasome in the EOC cell line; after treatment with LPS and ATP, the levels of cleaved IL-1β (p17) and caspase-1 (p20) increased ($p < 0.0001$, Figure 3b); however, MCC950 significantly inhibited their expression. Interestingly, PD-L1 expression also increased after LPS and ATP stimulation, but this was counteracted by subsequent MCC950 treatment ($p < 0.0001$, Figure 3b). Curiously, NLRP3 protein levels were not significantly changed.

NLRP3 Inflammasome Promoted Cell Proliferation in vitro

Next, we investigated the effect of the NLRP3 inflammasome on the proliferative capacity of the SKOV3 cell line. Cells were divided into three groups: a negative control, an LPS+ATP group, and an LPS+ATP+MCC950 group. All groups were cultured under identical conditions. The LPS+ATP group showed enhanced colony formation compared to the control, while the MCC950-treated group exhibited reduced colony numbers ($p < 0.05$, Figure 3c). TUNEL analysis showed that the LPS+ATP group had decreased apoptosis compared to the control, whereas the MCC950-treated group had increased apoptosis ($p < 0.0001$, Figure 3d). These findings suggest that LPS+ATP may enhance the self-renewal potential of SKOV3 cells in vitro, while MCC950 inhibited proliferation and promoted apoptosis.

Blocking NLRP3 Inflammasome in vivo Suppresses the Progress of EOC and Reduces the Expression of PD-L1

To assess the impact of the NLRP3 inflammasome on ovarian cancer in vivo, we established a subcutaneous syngeneic tumor model. Mice were divided into experimental and control groups and treated with MCC950 ($n=3$) or PBS ($n=3$), respectively (Figure 4a). After 19 days, mice were euthanized, and tissue samples were collected. Results showed significantly slower tumor growth in the experimental group ($p < 0.05$, Figure 4b–e), indicating that MCC950 inhibited tumor expansion by blocking the NLRP3 inflammasome. This confirmed that the NLRP3 inflammasome facilitated ovarian cancer growth in vivo and that its suppression could manage tumor progression.

In addition, mice treated with MCC950 showed significantly reduced levels of IL-1β (p17) in serum and tumor tissues ($p < 0.01$, Figure 4f and g), as well as decreased levels of cleaved caspase-1 (p20) in tissues ($p < 0.0001$, Figure 4h). These results indicated that MCC950 effectively inhibited NLRP3 inflammasome activation and mitigated the inflammatory environment in vivo. Meanwhile, MCC 950 reduced the expression of PD-L1 protein in tumor tissues ($p < 0.0001$, Figure 4i). This suggested that NLRP3 inflammasomes might exert a similar regulatory influence on PD-L1 in vivo. Consequently, blocking NLRP3 inflammasomes could potentially suppress the expression of PD-L1.

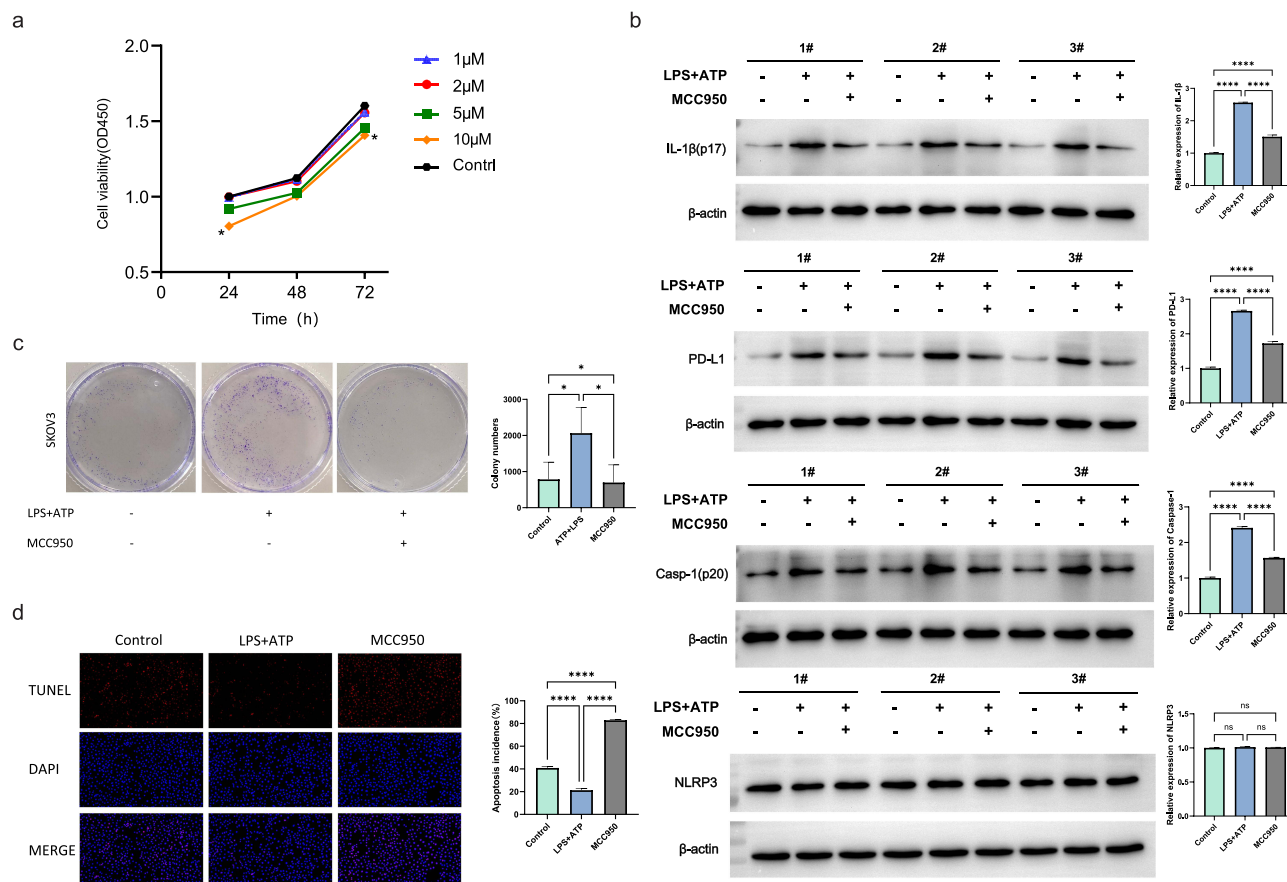


Figure 3 NLRP3 inflammasome promotes PD-L1 expression and cell proliferation in SKOV3 cell line. (a) Inhibition of the NLRP3 inflammasome reduced the proliferation rate of SKOV3 cells, as analyzed by CCK-8 assays. (b) Western blot analysis was performed to measure IL-1 β (p17), caspase-1 (p20), PD-L1, and NLRP3 under different treatments with LPS (6h) +ATP (1h) and/or MCC950 (1h) in the SKOV3 cell line. (c and d) Representative images of Colony formation(c) and TUNEL analysis(d) of SKOV3 cells under different treatment conditions were shown. Semi-quantitative analysis of colony numbers and apoptosis percentage were also included. Data were presented as mean \pm SD from three independent experiments. ns, no significance, *, $p < 0.05$, ****, $p < 0.0001$. "#" represents each independent experiment.

Blocking NLRP3 Inflammasome in vivo Decreased Immunosuppressive Cell Populations in EOC

Considering that NLRP3 inflammasome activation enhanced PD-L1 expression, which was involved in the immune escape, we hypothesized that this activation might impact the immune response and promote tumor growth. To test this, we analyzed immune cell populations in mice tissue samples. The results revealed that treatment with MCC950 significantly decreased the percentage of PD-1⁺ CD4⁺ T cells in tumor tissues ($p < 0.001$, Figure 5a), a similar trend was observed in the spleen, although without statistical significance. Concurrently, MCC950-treated mice showed reduced tumor-infiltrating CD8⁺ T cells and CD4⁺ T cells in tumor tissues ($p < 0.001$, Figure 5b and c). Additionally, inhibiting the NLRP3 inflammasome resulted in a significant decrease in the percentage of CD11b⁺ LY6G⁺ MDSC within tumor tissue ($p < 0.0001$, Figure 5d), along with reduced CXCL2 protein levels ($p < 0.0001$, Figure 5g). Studies indicate that migration of PMN-MDSC is linked to the chemokine receptor CXCR2 and its specific binding ligands, including CXCL2 and CXCL5.²⁷ Our findings implied that CXCL2 modulation by the NLRP3 inflammasome could critically impact MDSC population dynamics. Moreover, a significant decrease of TAM (CD 11b⁺ F4/80⁺) cell populations was observed in tumor tissues of MCC950-treated mice ($p < 0.01$, Figure 5e). However, there was no significant change in the regulatory T cells (Treg) percentage (Figure 5f); and none of the above cells percentages were significantly altered in the mice spleen tissue. In summary, blocking NLRP3 inflammasome partially improved the immunosuppressive status of the ovarian cancer TME.

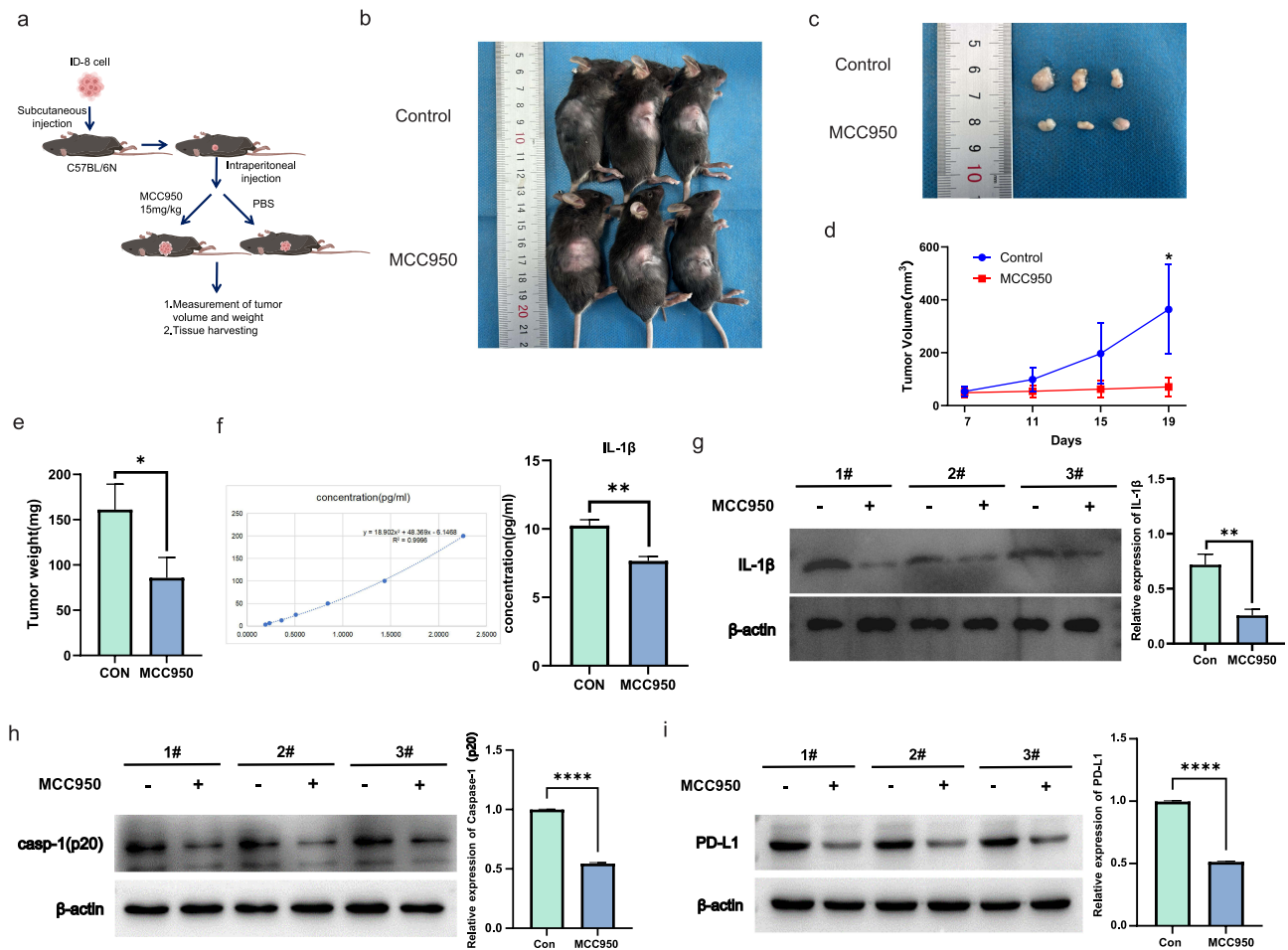


Figure 4 MCC950 application suppressed the activation of the NLRP3 inflammasome and slowed the progression of EOC in vivo. (a) Diagram illustrating the establishment of the murine model and the therapeutic intervention approaches. (b–c) Macroscopic tumor appearance across PBS-treated (n=3) and MCC950-treated (n=3) mice. (d) Tumor volume progression during the treatment period. (e) Comparison of the final tumor weight. (f–g) The levels of IL-1 β (p17) in the serum (f) and tumor tissues (g) of control and MCC950-treated mice were quantified by ELISA (f) and Western blot (g), respectively. (h–i) The protein levels of caspase-1 (p20) (h) and PD-L1 (i) in the tumor tissues of the mice from control and MCC950-treated groups were assessed by Western blot. All numerical data are represented as the mean \pm SD from at least three independent experimental repetitions. *, $p < 0.05$, **, $p < 0.01$, ****, $p < 0.0001$. n = biologically independent mouse samples. “#” represents each independent experiment.

Discussion

Malignant tumors are among the leading causes of death worldwide.²⁸ Notably, ovarian cancer is being increasingly diagnosed in younger women²⁹ and has a higher mortality rate than cervical and endometrial cancer.³⁰ Chronic inflammation can stimulate cell proliferation and the accumulation of reactive oxygen species,³¹ potentially facilitating tumorigenesis.³² The NLRP3 inflammasome contributes to creating an inflammatory environment³³ and plays a multifaceted role in tumor progression.³⁴ Its specific impact on ovarian cancer warrants further investigation. Here, we found that NLRP3 expression levels were elevated in EOC specimens, and patients with higher NLRP3 expression had poorer prognoses, indicating a significant role for NLRP3 in EOC progression.

The high heterogeneity of ovarian cancer primarily manifests through its intricate tumor microenvironment (TME). It has been demonstrated that NLRP3 can collaborate with its effector cytokines to promote an immunosuppressive TME within tumors.³⁵ GSEA analysis verified that NLRP3 overexpression was associated with an inverse relationship with inflammatory responses and the KRAS and other signaling pathways, indicating a potential inhibitory role in immune responses. The ESTIMATE algorithm suggested that increased NLRP3 expression enhanced immune infiltration and immunoreactivity in EOC. Typically, heightened immunoreactivity indicates a stronger tumor-killing effect. This contrasts with the findings from the GSEA and survival analyses, which may stem from the complex TME of ovarian cancer and immune escape triggered by overexpression of immune checkpoints.³⁶ Research has demonstrated that

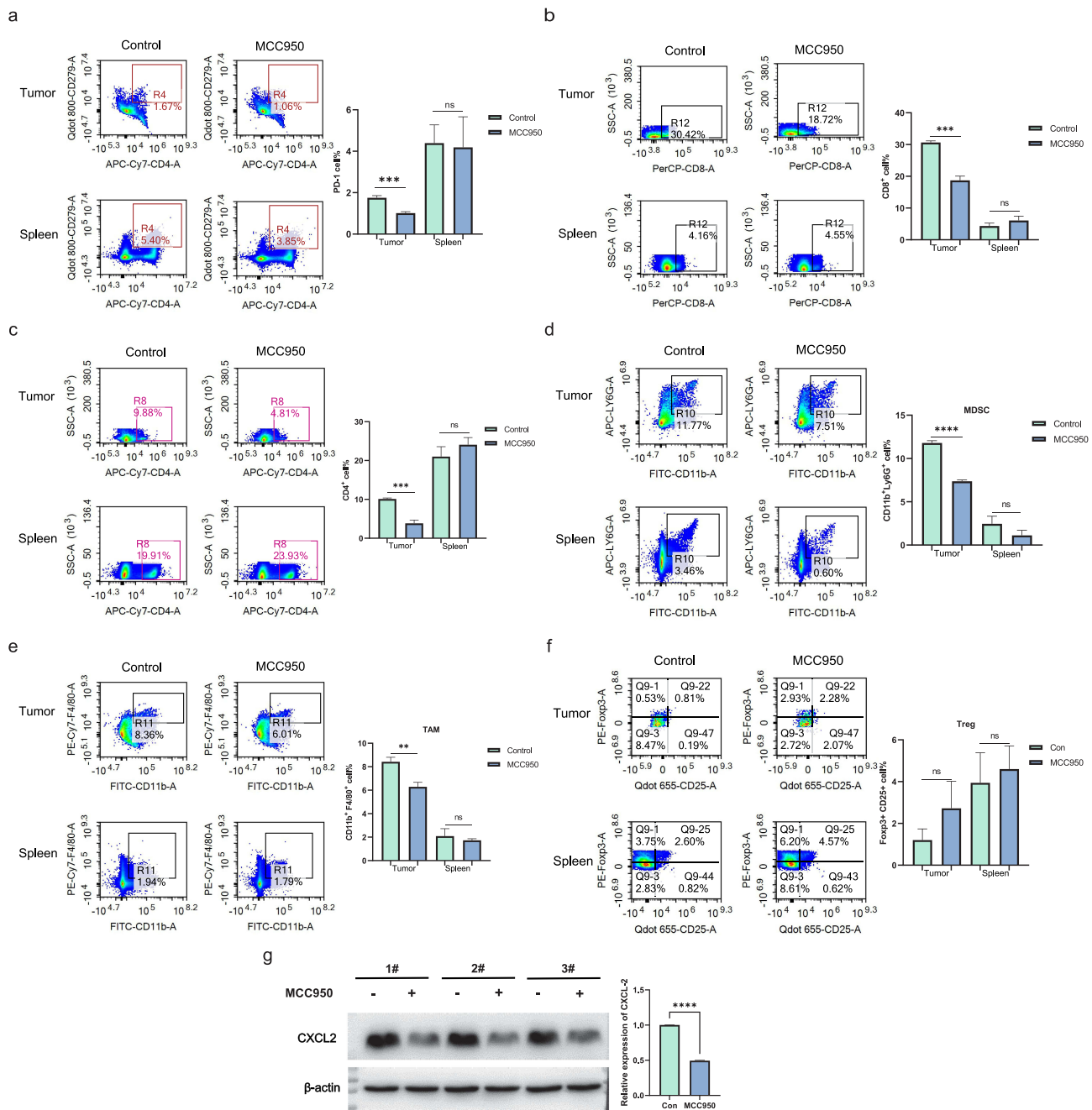


Figure 5 Inhibition of the NLRP3 inflammasome leads to a decrease in immunosuppressive cells in murine ovarian cancer. (a–c) Flow cytometry analysis of PD-1⁺ CD4⁺ T cells (a), effector CD8⁺ (b) and CD4⁺ (c) T cells in spleens and tumors of mice treated with PBS (as control) or MCC950, and their quantification and statistical evaluation. (d–f) Representative flow cytometry graphs (left panel) and bar charts (right panel) demonstrating the frequencies and statistical evaluation of MDSCs (d), TAMs (e), and Tregs (f) in the tumor and spleen of control and MCC950-treated mice. (g) Analysis of CXCL2 protein expression in murine tumor tissues under different treatment conditions with and without MCC950 using Western blot. (All quantitative data are presented as mean \pm SD from at least three biologically independent experiments, ns, no significance. **, $p < 0.01$, ***, $p < 0.001$, ****, $p < 0.0001$). “#” represents each independent experiment.

NLRP3 is linked to various immune checkpoints,²⁶ and a correlation between PD-L1 and NLRP3 was identified in interferon- γ (IFN- γ)-induced myotubes.³⁷ Our findings support a positive correlation between NLRP3 and immune checkpoints like PD-L1 in EOC, consistent with prior observations. This correlation was validated in the SKOV3 cell line, suggesting potential interactive mechanisms between NLRP3 and PD-L1.

The NLRP3 inflammasome, upon activation, converts pro-caspase-1 into active caspase-1(p20), which then triggers the conversion of pro-IL-1 β into IL-1 β (p17).³⁸ This study confirmed that LPS combined with ATP could activate the

NLRP3 inflammasome in EOC cells, enhancing the expression of caspase-1 (p20) and IL-1 β (p17). However, this enhancement could be suppressed by MCC950 without altering the NLRP3 protein level. This may be attributed to MCC950's mechanism of obstructing the oligomerization of ASCs, thereby preventing inflammasome activation.³⁹ Furthermore, activation of the NLRP3 inflammasome could promote EOC cell proliferation, which might be associated with inflammatory mediators like IL-1 β induced by the NLRP3 inflammasome. Excessive IL-1 β is considered a factor that promotes tumor growth.⁴⁰ In particular, *in vivo* studies showed significantly higher IL-1 β levels in control mice's serum and tumor tissues compared to MCC950-treated mice, with faster tumor progression.

In addition, activation of the NLRP3 inflammasome increased PD-L1 expression, whereas MCC950 significantly downregulated PD-L1 by blocking the NLRP3 inflammasome both *in vitro* and *in vivo*, and also slowed tumor growth. Considering the pivotal role of PD-L1/ PD-1 in tumor immune evasion, the progression impediment of EOC induced by NLRP3 inflammasome inhibition may be associated with changes in the immunosuppressive state. Moreover, our results indicated a reduction in exhausted T cells in MCC950-treated mice, particularly the proportion of PD-1⁺ CD4⁺ T cells in tumor tissues, suggesting that blocking NLRP3 inflammasome could reduce immune evasion. Additionally, it is noteworthy that the inhibition of NLRP3 activity also led to a reduction in CD8⁺ T cells, which might partially impair the cytotoxic function of T cells; Nevertheless, analysis from Tengedal et al⁴¹ in a melanoma model suggests that the inhibition of NLRP3 does not directly affect T cell cytotoxicity but rather improves the immunosuppressive environment by limiting the expansion of MDSCs. This could indirectly enhance overall anti-tumor responses. Given the limited number of subjects in these studies, and differential roles of NLRP3 across various cancers,⁷ further in-depth research is needed to clarify whether NLRP3 inhibition directly or indirectly influences CD8⁺ T cell activity and its subsequent effects on tumor progression.

Expansion of MDSCs typically occurs in chronic inflammation⁴² and plays a critical role in immuno-suppression in cancer.^{18,19} MDSC migration can be regulated by CXCL2-CXCR2 interaction.²⁷ In the current study, treatment with MCC950 reduced MDSC percentage and CXCL2 expression in mice tissues, suggesting that NLRP3 inflammasome may modulate MDSC activity via CXCL2, although the precise mechanism remains unclear. MDSCs are also thought to regulate cancer stem cells (CSCs), enhancing the ovarian cancer and multiple myeloma stemness.^{43,44} It remains to be investigated whether the heightened clone formation of SKOV3 cells induced by the NLRP3 inflammasome (Figure 3c) is linked to MDSCs. TAMs are critical for inflammation promotion and immune response modulation, correlate with adverse cancer outcomes.⁴⁵ They are major producers of IL-1 β .⁴⁶ Our research demonstrated that MCC950 treatment mice exhibited a significantly reduced proportion of TAMs and IL-1 β levels. Treg cells facilitate immune evasion,⁴⁷ but this study did not observe any ameliorative impact of MCC950 treatment on this cell subset. This study demonstrated that MCC950 induced apoptosis in SKOV3 cells (Figure 3d), which could be partially attributed to immune cell remodeling following NLRP3 inhibition. In addition, silencing NLRP3 has been shown in liver cancer to downregulate the anti-apoptotic protein BCL-2 and upregulate the pro-apoptotic protein Bax.⁴⁸ Furthermore, CXCL2, a chemokine influenced by NLRP3 activity, stimulates BCL-2 transcription while inhibiting Bax transcription, thus exerting an anti-apoptotic effect.⁴⁹ These findings indicate that the apoptotic effects of MCC950 are complex, involving not only the reduction of immune-suppressive mechanisms associated with NLRP3 signaling but also potentially direct pro-apoptotic effects on tumor cells via NLRP3 and/or CXCL2 signaling. Further research is needed to elucidate the relative contributions of these mechanisms in ovarian cancer.

However, this study has certain limitations that should be acknowledged. We chose the murine subcutaneous tumor model for its practicality and direct observation of drug effects on tumor tissue. However, this model did not fully replicate the ovarian cancer TME due to the use of a non-orthotopic ovarian model. This may explain why significant changes in the immune cell population were observed only in the tumor tissue, rather than in the spleen tissue. Additionally, due to the highly immunosuppressive environment of ovarian cancer, current immunotherapies have shown limited success and have not significantly improved survival outcomes.^{50,51} This underscores the challenges in developing effective immune-oncologic treatments for ovarian cancer. However, activating the immune system remains a promising strategy for overcoming these barriers.⁵² Our study demonstrates that targeting NLRP3 can alleviate the immunosuppressive state of ovarian cancer, offering a novel and forward-looking approach. Further investigation is

needed to evaluate the combined effects and mechanisms of targeting NLRP3 with immunotherapy, which may provide insights into enhancing anti-ovarian cancer immune responses.

Conclusion

In summary, the NLRP3 inflammasome promotes an inflammatory environment that enhances EOC proliferation and creates an immunosuppressive TME. Blocking NLRP3 inflammasome could largely mitigate the immunosuppressive environment and inhibit tumor growth. The NLRP3 inflammasome represents a promising therapeutic target for EOC, offering novel insights into ovarian cancer treatment.

Abbreviations

NLRP3, Nod-like receptor protein 3; PD-L1, Programmed death-ligand 1; EOC, Epithelial ovarian cancer; TME, Tumor microenvironment; LPS, Lipopolysaccharide; RT, Room temperature; MDSCs, Myeloid-derived suppressor cells; TAMs, Tumor-associated macrophages; Tregs, Regulatory T cells.

Data Sharing Statement

The datasets generated during and/or analysed during the current study are available in the [UCSC Xena] repository, [https://xenabrowser.net/datapages/?dataset=TCGA-OV.htseq_counts.tsv&host=https%3A%2F%2Fgdc.xenahubs.net&removeHub=https%3A%2F%2Fxena.treehouse.gi.ucsc.edu%3A443].

Ethics Approval and Informed Consent

The human study was conducted in accordance with the principles of the Declaration of Helsinki and was approved by the Ethics Committee of the Second Affiliated Hospital of Harbin Medical University under approval number YJSKY2022-074. The animal study was also approved by the same committee under approval number YJSDW2022-058. Informed consent was obtained from all individual participants included in the study.

Consent to Publish

The authors affirm that the details of any images, recordings, etc can be published, and that the persons providing consent have been shown the article contents to be published.

Author Contributions

All authors contributed to the study conception and design. Material preparation, data collection and analysis were performed by Wenjing Pan, Zhaoyang Jia and Jingtong Du. The first draft of the manuscript was written by Wenjing Pan and all authors commented on previous versions of the manuscript. All authors read and approved the final manuscript”.

Funding

The authors declare that no funds, grants, or other support were received during the preparation of this manuscript.

Disclosure

The authors have no relevant financial or non-financial interests to disclose.

References

1. Baczewska M, Bojczuk K, Kolakowski A, Dobroch J, Guzik P, Knapp P. Obesity and energy substrate transporters in ovarian cancer-review. *Molecules*. 2021;26(6):1659. doi:10.3390/molecules26061659
2. Siegel RL, Giaquinto AN, Jemal A. Cancer statistics, 2024. *CA Cancer J Clin*. 2024;74(1):12–49. doi:10.3322/caac.21820
3. Pankowska KA, Będkowska GE, Chociej-Stypułkowska J, Rusak M, Dąbrowska M, Osada J Crosstalk of immune cells and platelets in an ovarian cancer microenvironment and their prognostic significance. *Int J Mol Sci*. 2023;24(11).
4. Zhang Q, Ding J, Wang Y, He L, Xue F. Tumor microenvironment manipulates chemoresistance in ovarian cancer (Review). *Oncol Rep*. 2022;47(5). doi:10.3892/or.2022.8313
5. Weeden CE, Hill W, Lim EL, Gronroos E, Swanton C. Impact of risk factors on early cancer evolution. *Cell*. 2023;186(8):1541–1563. doi:10.1016/j.cell.2023.03.013

6. Kisielewski R, Tołwińska A, Mazurek A, Ludański P. Inflammation and ovarian cancer--current views. *Ginekol Pol.* 2013;84(4):293–297. doi:10.17772/gp/1579
7. Karki R, Kanneganti TD. Diverging inflammasome signals in tumorigenesis and potential targeting. *Nat Rev Cancer.* 2019;19(4):197–214. doi:10.1038/s41568-019-0123-y
8. Cullen SP, Kearney CJ, Clancy DM, Martin SJ. Diverse activators of the NLRP3 inflammasome promote IL-1beta secretion by triggering necrosis. *Cell Rep.* 2015;11(10):1535–1548. doi:10.1016/j.celrep.2015.05.003
9. Kelley N, Jeltema D, Duan Y, He Y. The NLRP3 inflammasome: an overview of mechanisms of activation and regulation. *Int J Mol Sci.* 2019;20(13):3328. doi:10.3390/ijms20133328
10. He Y, Hara H, Nunez G. Mechanism and regulation of NLRP3 inflammasome activation. *Trends Biochem Sci.* 2016;41(12):1012–1021. doi:10.1016/j.tibs.2016.09.002
11. Sharma D, Kanneganti TD. The cell biology of inflammasomes: mechanisms of inflammasome activation and regulation. *J Cell Biol.* 2016;213(6):617–629. doi:10.1083/jcb.201602089
12. Wei Q, Mu K, Li T. Deregulation of the NLRP3 inflammasome in hepatic parenchymal cells during liver cancer progression. *Lab Invest.* 2014;94(1):52–62. doi:10.1038/labinvest.2013.126
13. Allen IC, TeKippe EM, Woodford RM, et al. The NLRP3 inflammasome functions as a negative regulator of tumorigenesis during colitis-associated cancer. *J Exp Med.* 2010;207(5):1045–1056. doi:10.1084/jem.20100050
14. Karki R, Man SM, Kanneganti TD. Inflammasomes and Cancer. *Cancer Immunol Res.* 2017;5(2):94–99. doi:10.1158/2326-6066.CIR-16-0269
15. Chen Y, Li ZY, Zhou GQ, Sun Y. An immune-related gene prognostic index for head and neck squamous cell carcinoma. *Clin Cancer Res.* 2021;27(1):330–341. doi:10.1158/1078-0432.CCR-20-2166
16. Theivanthiran B, Evans KS, DeVito NC. A tumor-intrinsic PD-L1/NLRP3 inflammasome signaling pathway drives resistance to anti-PD-1 immunotherapy. *J Clin Invest.* 2020;130(5):2570–2586. doi:10.1172/JCI133055
17. Papafraqos I, Grigoriou M, Boon L, Kloetgen A, Hatzioannou A, Verginis P. Ablation of NLRP3 inflammasome rewires MDSC function and promotes tumor regression. *Front Immunol.* 2022;13:889075. doi:10.3389/fimmu.2022.889075
18. Veglia F, Sanseviero E, Gabrilovich DI. Myeloid-derived suppressor cells in the era of increasing myeloid cell diversity. *Nat Rev Immunol.* 2021;21(8):485–498. doi:10.1038/s41577-020-00490-y
19. Hegde S, Leader AM, Merad M. MDSC: markers, development, states, and unaddressed complexity. *Immunity.* 2021;54(5):875–884. doi:10.1016/j.immuni.2021.04.004
20. Zhu Y, Chen P, Hu B. MDSC-targeting gold nanoparticles enhance PD-1 tumor immunotherapy by inhibiting NLRP3 inflammasomes. *Biomaterials.* 2024;307:122533. doi:10.1016/j.biomaterials.2024.122533
21. Chang CM, Wang ML, Lu KH, et al. Integrating the dysregulated inflammasome-based molecular functionome in the malignant transformation of endometriosis-associated ovarian carcinoma. *Oncotarget.* 2018;9(3):3704–3726. doi:10.18632/oncotarget.23364
22. Su KM, Wang PH, Yu MH, Chang CM, Chang CC. The recent progress and therapy in endometriosis-associated ovarian cancer. *J Chin Med Assoc.* 2020;83(3):227–232. doi:10.1097/JCMA.0000000000000262
23. Yoshihara K, Shahmoradgoli M, Martinez E, et al. Inferring tumour purity and stromal and immune cell admixture from expression data. *Nat Commun.* 2013;4:2612. doi:10.1038/ncomms3612
24. Roby KF, Taylor CC, Sweetwood JP, et al. Development of a syngeneic mouse model for events related to ovarian cancer. *Carcinogenesis.* 2000;21(4):585–591. doi:10.1093/carcin/21.4.585
25. Coll RC, Robertson AA, Chae JJ, et al. A small-molecule inhibitor of the NLRP3 inflammasome for the treatment of inflammatory diseases. *Nat Med.* 2015;21(3):248–255. doi:10.1038/nm.3806
26. Ding Y, Yan Y, Dong Y. NLRP3 promotes immune escape by regulating immune checkpoints: a pan-cancer analysis. *Int Immunopharmacol.* 2022;104:108512. doi:10.1016/j.intimp.2021.108512
27. Shi H, Han X, Sun Y, et al. Chemokine (C-X-C motif) ligand 1 and CXCL2 produced by tumor promote the generation of monocytic myeloid-derived suppressor cells. *Cancer Sci.* 2018;109(12):3826–3839. doi:10.1111/cas.13809
28. Timar J, Kashofer K. Molecular epidemiology and diagnostics of KRAS mutations in human cancer. *Cancer Metastasis Rev.* 2020;39(4):1029–1038. doi:10.1007/s10555-020-09915-5
29. Lheureux S, Gourley C, Vergote I, Oza AM. Epithelial ovarian cancer. *Lancet.* 2019;393(10177):1240–1253. doi:10.1016/S0140-6736(18)32552-2
30. Kuroki L, Guntupalli SR. Treatment of epithelial ovarian cancer. *BMJ.* 2020;371:m3773. doi:10.1136/bmj.m3773
31. Grivennikov SI, Greten FR, Karin M. Immunity, inflammation, and cancer. *Cell.* 2010;140(6):883–899. doi:10.1016/j.cell.2010.01.025
32. Rokavec M, Oner MG, Hermeking H. Inflammation-induced epigenetic switches in cancer. *Cell Mol Life Sci.* 2016;73(1):23–39. doi:10.1007/s00018-015-2045-5
33. Martinon F, Burns K, Tschopp J. The inflammasome: a molecular platform triggering activation of inflammatory caspases and processing of proIL-beta. *Mol Cell.* 2002;10(2):417–426. doi:10.1016/S1097-2765(02)00599-3
34. Lin TY, Tsai MC, Tu W, et al. Role of the NLRP3 inflammasome: insights into cancer hallmarks. *Front Immunol.* 2020;11:610492. doi:10.3389/fimmu.2020.610492
35. Moossavi M, Parsamanesh N, Bahrami A, Atkin SL, Sahebkar A. Role of the NLRP3 inflammasome in cancer. *Mol Cancer.* 2018;17(1):158. doi:10.1186/s12943-018-0900-3
36. Vanichapol T, Chutipongtanate S, Anurathapan U, Hongeng S. Immune escape mechanisms and future prospects for immunotherapy in neuroblastoma. *Biomed Res Int.* 2018;2018:1812535. doi:10.1155/2018/1812535
37. Ding M, Huang T, Zhu R. Immunological behavior analysis of muscle cells under IFN-gamma stimulation in vitro and in vivo. *Anat Rec.* 2018;301(9):1551–1563. doi:10.1002/ar.23834
38. Huang CF, Chen L, Li YC, et al. NLRP3 inflammasome activation promotes inflammation-induced carcinogenesis in head and neck squamous cell carcinoma. *J Exp Clin Cancer Res.* 2017;36(1):116. doi:10.1186/s13046-017-0589-y
39. Li H, Guan Y, Liang B, et al. Therapeutic potential of MCC950, a specific inhibitor of NLRP3 inflammasome. *Eur J Pharmacol.* 2022;928:175091. doi:10.1016/j.ejphar.2022.175091
40. Caronni N, La Terza F, Vittoria FM. IL-1beta(+) macrophages fuel pathogenic inflammation in pancreatic cancer. *Nature.* 2023;623(7986):415–422. doi:10.1038/s41586-023-06685-2

41. Tengesdal IW, Menon DR, Osborne DG, et al. Targeting tumor-derived NLRP3 reduces melanoma progression by limiting MDSCs expansion. *Proc Natl Acad Sci U S A*. 2021;118(10).
42. Millrud CR, Bergenfelz C, Leandersson K. On the origin of myeloid-derived suppressor cells. *Oncotarget*. 2017;8(2):3649–3665. doi:10.18632/oncotarget.12278
43. Cui T, Kryczek I, Zhao L. Myeloid-derived suppressor cells enhance stemness of cancer cells by inducing microRNA101 and suppressing the corepressor CtBP2. *Immunity*. 2013;39(3):611–621. doi:10.1016/j.immuni.2013.08.025
44. Ai L, Mu S, Sun C. Myeloid-derived suppressor cells endow stem-like qualities to multiple myeloma cells by inducing piRNA-823 expression and DNMT3B activation. *Mol Cancer*. 2019;18(1):88. doi:10.1186/s12943-019-1011-5
45. Baer JM, Zuo C, Kang LI, et al. Fibrosis induced by resident macrophages has divergent roles in pancreas inflammatory injury and PDAC. *Nat Immunol*. 2023;24(9):1443–1457. doi:10.1038/s41590-023-01579-x
46. Bill R, Wirapati P, Messemaker M, et al. CXCL9: SPP1 macrophage polarity identifies a network of cellular programs that control human cancers. *Science*. 2023;381(6657):515–524. doi:10.1126/science.ade2292
47. Tay C, Tanaka A, Sakaguchi S. Tumor-infiltrating regulatory T cells as targets of cancer immunotherapy. *Cancer Cell*. 2023;41(3):450–465. doi:10.1016/j.ccell.2023.02.014
48. Liu W, Zhang F, Quan B, et al. NLRP3/IL-1beta induced myeloid-derived suppressor cells recruitment and PD-L1 upregulation promotes oxaliplatin resistance of hepatocellular carcinoma. *MedComm*. 2023;4(6):e447. doi:10.1002/mco2.447
49. Wang HC, Haung LY, Wang CJ, et al. Tumor-associated macrophages promote resistance of hepatocellular carcinoma cells against sorafenib by activating CXCR2 signaling. *J Biomed Sci*. 2022;29(1):99. doi:10.1186/s12929-022-00881-4
50. Odunsi K. Immunotherapy in ovarian cancer. *Ann Oncol*. 2017;28(suppl_8):viii1–viii7. doi:10.1093/annonc/mdx444
51. Li Y, Gao Y, Zhang X, Guo H, Gao H. Nanoparticles in precision medicine for ovarian cancer: from chemotherapy to immunotherapy. *Int J Pharm*. 2020;591:119986. doi:10.1016/j.ijpharm.2020.119986
52. Chiang CL, Rovelli R, Sarivalasis A, Kandalafi LE. Integrating cancer vaccines in the standard-of-care of ovarian cancer: translating preclinical models to human. *Cancers*. 2021;13(18):4553. doi:10.3390/cancers13184553

ImmunoTargets and Therapy

Dovepress

Publish your work in this journal

ImmunoTargets and Therapy is an international, peer-reviewed open access journal focusing on the immunological basis of diseases, potential targets for immune based therapy and treatment protocols employed to improve patient management. Basic immunology and physiology of the immune system in health, and disease will be also covered. In addition, the journal will focus on the impact of management programs and new therapeutic agents and protocols on patient perspectives such as quality of life, adherence and satisfaction. The manuscript management system is completely online and includes a very quick and fair peer-review system, which is all easy to use. Visit <http://www.dovepress.com/testimonials.php> to read real quotes from published authors.

Submit your manuscript here: <http://www.dovepress.com/immunotargets-and-therapy-journal>